

IMI2 Project ID 101005077

CARE – Corona Accelerated R&D in Europe

WP6 – From lead to pre-clinical candidate and proof-of-concept in small-animal and non-human primate models

6.2 Report on suitability of mouse-adapted SARS CoV-2 virus for lethal humanised ACE-2 model

Lead contributor	P21-EDI-IVI
Other contributors	

Document History

Version	Date	Description
6.2.1	06 Apr 2021	Version signed off by IVI

Table of Contents

Introduction	3
Methods	4
Synthetic Viruses	4
In vivo Model	5
Ethics and biosafety	5
Animals	5
In vivo infection	5
Histological analysis	5
Study groups	6
Outcome Parameters/ Readout	6
Humane endpoints:	7
Results	7
MA-SARS-CoV-2 virus	8
MA10-SARS-CoV-2 virus	8
Discussion	9
Conclusion	10
References	10



Introduction

SARS-CoV-2 first appeared in the human population at the end of 2019 in Wuhan, China and has since infected 127 million people worldwide by the beginning of April 2021. It is unclear how it adapted to humans although it is thought to have originated in bats and then passed through an unknown intermediate animal host before infecting humans. Strict measures were introduced with varying success across the world including limiting travel, implementing lockdowns, and “track and trace” to follow the spread of the disease. Since the beginning of 2021, the first vaccines have been rolled out and are already contributing to the control of the pandemic with reduced hospitalisations in vaccinated age groups.

In the “fight against the virus”, animal models play a key role in the development of prophylactic vaccines and therapeutic antivirals. These models ideally mimic the human response towards the virus in terms of toxicity, safety and efficacy profiles and should reproduce viral replication as well as the clinical outcome observed in patients. Within this report, we describe a mouse model with potential for future testing of antiviral prophylactics and therapeutic compounds.

SARS-CoV-2 uses human Angiotensin-Converting Enzyme (hACE2) as the entry receptor to bind and enter cells. The differences between the mouse and human receptor mean that inbred mice do not support high titre viral replication as mouse ACE2 does not effectively bind the viral spike protein. This is the main impediment when trying to infect mouse cells with SARS-CoV-2. Several strategies have been developed to solve this problem. Due to the quasispecies nature of RNA viruses, adaptation is possible as rare viruses in the swarm containing beneficial mutations in the spike protein increase their binding affinity to mouse ACE2 and are expected to be selected owing to their higher levels of replication in mouse airways and lungs.

Reverse genetics has been used to modify the receptor-binding domain of the SARS-CoV-2 virus by adapting the spike protein to improve binding to the mouse ACE2 receptor so that it can infect mouse cells via the mouse ACE2 receptor. Specifically, the SARS CoV-2 Spike receptor-binding domain (RBD) was remodelled to facilitate efficient binding to mouse ACE2. Importantly Q498 was identified as being incompatible with mouse ACE2. Further molecular modelling of the SARS-CoV-2 Spike RBD-receptor interface suggested a loss of interaction between Q498 and Q42 of human ACE2 which may diminish binding efficiency. Residues Q498 and P499 were therefore substituted with Y and T, respectively, to restore the interaction. This virus was designated SARS CoV-2 MA (MA). Initial experiments using this strategy produced mice sensitive to infection, but they only developed mild symptoms [1].

The MA virus was made more pathogenic by serial passage *in vivo* in the lungs of young Balb/c mice. By passage 10, greater than 10% weight loss was observed 2 days post-infection. Sequencing identified in addition to the Q498Y and P499T mutation present in the parent MA virus, five additional nucleotide changes, resulting in nonsynonymous coding changes. These were located in nonstructural protein 4 (nsp4) (C9438T), nsp7 (A118447G), nsp8 (A12159G), spike (S; C23039A) and open reading frame 6 (ORF6; T27221C) [2]. This virus was designated MA10-SARS CoV-2 (MA10).

The hACE2 knock-in [3] and K18-hACE2 [4, 5] mouse models used in the CARE consortium described in deliverable D6.1 were genetically adapted to allow infection by SARS-CoV-2. It is also important to define an alternative approach where the virus is adapted to the mice, rather than genetically adapting the mice to interact with the virus.

To this end, this deliverable aims to assess the suitability of mouse-adapted SARS CoV-2 viruses as a lethal mouse model.

Methods

Synthetic Viruses

To produce mouse-adapted SARS-CoV-2 viruses for our studies we took into consideration 3R principles. To avoid subjecting animals to serial passaging and repeating studies already performed, we relied on published data to design our synthetic mouse-adapted virus mutants using data from a study where the SARS-CoV-2 Spike RBD was remodelled to facilitate binding to mouse ACE2 [1] and a subsequent in vivo passaging of SARS-CoV-2 in mice [2]. We have rescued 2 independent mouse-adapted clones, designated maSARS-CoV-2 and ma10SARS-CoV-2. The mutations were introduced by PCR mutagenesis (Table 1) to the pUC57 plasmid containing SARS-CoV-2 fragments using Q5® Site-Directed Mutagenesis Kit (New England BioLab). Infectious cDNA clones were then generated using the in-yeast TAR cloning method as described previously [3, 6]. In vitro transcription was performed for EagI-cleaved YACs and PCR-amplified SARS-CoV-2 N gene using the T7 RiboMAX Large Scale RNA production system (Promega). Transcribed capped mRNA was electroporated into baby hamster kidney (BHK-21) cells expressing SARS-CoV N protein. Electroporated cells were co-cultured with susceptible Vero E6 cells to produce passage 0 (P.0) of the recombinant viruses. Subsequently, progeny viruses were used to infect fresh Vero E6 cells to generate P.1 stocks for downstream experiments.

Table 1 Mutations introduced into SARS CoV-2 to generate mouse-adapted synthetic viruses

Virus	Genome Position	Gene	Nucleotide mutation	Amino mutation	Acid
MA-SARS-CoV-2	23,054	Spike	CAACCC > TACACG	Q > Y and P > T	
MA10-SARS-CoV-2	9,438	nsp4	C > T	T > I	
	11,847	nsp7	A > G	K > R	
	12,159	nsp8	A > G	E > G	
	23,039	Spike	C > A	Q > K	
	23,054	Spike	CAACCC > TACACG	Q > T and P > T	
	27,221	ORF6	T > C	F > S	

In vivo Model

Ethics and biosafety

Mouse experiments were conducted in compliance with the Swiss Animal Welfare legislation, and animal studies were reviewed and approved by the commission for animal experiments of the canton of Bern (License BE43/20). All procedures for the evaluation of mouse-adapted SARS-CoV-2 infection were carried out in the BSL-3 facility at the Institute of Virology and Immunology (Mittelhäusern) where mice were housed in individually HEPA-filtered cages (IsoCage N, Tecniplast).

Animals

Balb/c mice were obtained from Janvier Lab. All mice were maintained with a 12-h/12-h light/dark cycle, 22 ± 1 °C ambient temperature and $50 \pm 5\%$ humidity, autoclaved acidified water, autoclaved cages including food, bedding, and environmental enrichment.

In vivo infection

Mice were anaesthetised with isoflurane and infected intranasally with 40 μ l (i.e., 20 μ l per nostril) of MA-SARS-CoV-2, MA10-SARS-CoV-2, or mock culture medium. Animals were monitored daily for weight loss, the severity of clinical signs and survival. Throat swabs were collected every two days under brief isoflurane anaesthesia using ultrafine sterile flock swabs (Hydraflock, Puritan, 25-3318-H). The tips of the swabs were placed in 0.5 ml of RA1 lysis buffer (Macherey-Nagel, ref. 740961) supplemented with 1% β -mercaptoethanol and vortexed. At selected time points or once the humane endpoint was reached (see below for details), blood was collected and the mice euthanised for organ harvest. Systematic tissue sampling was performed: the lung left lobe was fixed in 10% neutral buffered formalin; the lung right superior lobe was collected for RNA isolation in RA1 lysis buffer supplemented with 1% β -mercaptoethanol; the lung middle, inferior and post-caval lobes were collected in DMEM in gentleMACS M Tubes (Miltenyi Biotec, 130-096-335). Moreover, the right nasal conchae, right olfactory bulb and part of the right brain hemisphere were collected for RNA isolation, while the left nasal conchae were collected in DMEM in gentleMACS M Tubes. Tissue processing and RT-PCR for the viral E gene were carried out as previously described [3].

Histological analysis

Fixed tissue samples were processed, sectioned and stained with haematoxylin and eosin (H&E) by the COMPATH core facility (University of Bern). Histopathological lung slides were examined by a board-certified veterinary pathologist, who was blinded to the identity of the samples. The following parameters were evaluated following a scheme adapted from [7]: lesion distribution and percentage of affected lung tissue; degree of interstitial, peribronchiolar, perivascular, and intra-alveolar inflammation; necrosis of the alveolar wall and the bronchiolar epithelium; alveolar and perivascular oedema; and vascular lesions, namely endothelial activation, inflammation, and vascular wall necrosis.

Study groups

Mice were acclimated for 7 days prior to infection and divided into different groups for infection with the two synthetic clones of mouse-adapted SARS-CoV-2 (i.e. MA and MA10) at the specified plaque-forming unit (PFU)/mouse (Table 2). Mock infections were carried out with DMEM alone to serve as controls. Viral dose for infection was determined based on published data [1, 2].

Table 2: Description of the experimental groups.

Group	Mouse strain – Sex - Age	Mouse-adapted virus	Dose	N
1	BALB/c - Female – 6week old	mock	-	2
2	BALB/c - Female – 6week old	MA	1x10 ⁵ PFU/mouse	4
3	BALB/c - Female – 13week old	MA10	1x10 ⁵ PFU/mouse	4
4	BALB/c - Female – 14week old	MA10	1x10 ⁴ PFU/mouse	3
5	BALB/c - Female – 14week old	MA10	1x10 ³ PFU/mouse	2
6	BALB/c - Male – 14week old	MA10	5x10 ² PFU/mouse	4

Outcome Parameters/ Readout

Mice were observed daily and changes in body weight monitored. Clinical signs of disease were also noted using the scheme described in Table 3. Survival of the animal was defined by not reaching the humane endpoint. Sampling for viral loads was done by taking longitudinal throat swabs and harvesting organs at termination (day 4 p.i.) in lungs, brain and olfactory bulb. Virus load was measured by RT-qPCR on extracted total viral RNA, plaque assays from organ homogenates, lung histopathology and immunohistochemistry, as well as assessing cytokine levels in serum and organ homogenates.

Table 3: Description of Clinical Signs and Scoring System.

Observation	Description	Score
Motility and reaction time	• Mouse is normal, alert with spontaneous motility	0
	• Mouse shows spontaneous mobility but is slower than usual	1

	<ul style="list-style-type: none"> • Mouse shows moderate reduced activity • Mouse is not active unless stimulated by the experimenter • The mouse is lethargic and not moving upon gentle stimulation 	<p>2</p> <p>3</p> <p>4</p>
Fur	<ul style="list-style-type: none"> • Normal / Shining • Not clean / Matted • Ruffled 	<p>0</p> <p>1</p> <p>2</p>
Respiration	<ul style="list-style-type: none"> • Breathing normal • Breathing slightly changed • Laboured breathing 	<p>0</p> <p>1</p> <p>4</p>

Humane endpoints:

The animals are humanely sacrificed when reaching humane endpoints based on multiple criteria including bodyweight loss, posture, activity, grooming, mucosal secretions, and clinical signs as defined by the animal experimentation authorisation (BE43/20).

Results

To assess the suitability of mouse-adapted SARS-CoV-2 viruses as a lethal mouse model, Balb/c mice were infected intranasally with the synthetic clones of the MA- or MA10-SARS-CoV-2. A schematic representation of the experimental design is shown in Figure 1.

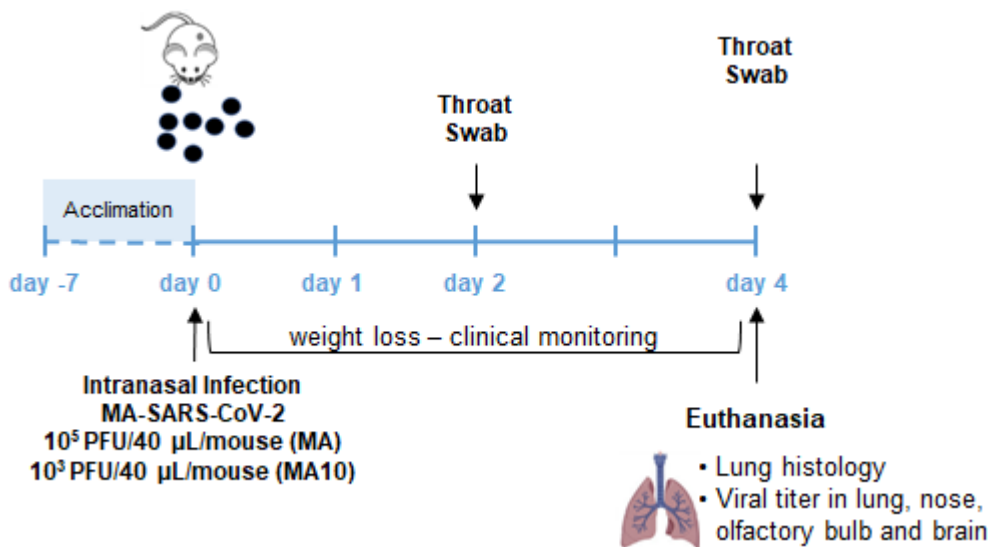


Figure 1: Experimental set-up and time schedule for the evaluation of clinical disease in mice infected with mouse-adapted SARS-CoV-2.



MA-SARS-CoV-2 virus

Mice did not show any clinical signs of infection or bodyweight loss in the four days following intranasal infection with 1×10^5 plaque-forming unit (PFU) of MA (Figure 2a). However, high-titre virus replication was observed in the lung of the mice four days after infection (Figure 2b).

Histologically, mice infected with MA-SARS-CoV-2 displayed mild to moderate, multifocal perivascular and peribronchiolar mononuclear infiltrates, which extended into the adjacent alveolar walls on day 4 post-infection (Figure 3b and e). Additionally, occasional vessels displayed a mild to moderate endothelial activation, with intraluminal and intramural accumulation of inflammatory cells. The bronchiolar epithelium was occasionally necrotic, and few macrophages were visible within the bronchiolar lumen.

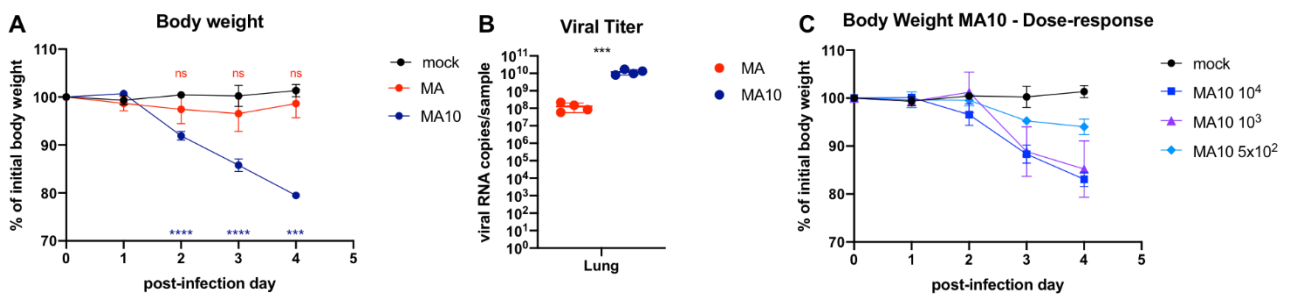


Figure 2: Evaluation of MA- and MA10-SARS-CoV-2 infection in Balb/c mice. A–B) Balb/c mice were mock-infected (black dots) or infected with 1×10^5 PFU MA-SARS-CoV-2 (red dots) or MA10-SARS-CoV-2 (red dots). A) Weight loss. ns: not significant, *** $p < 0.001$, **** $p < 0.0001$ by student t-test as compared to the mock-infected group. B) Viral titre in lungs 4 days post-infection as determined by qPCR. *** $p < 0.001$ by student t-test. C) Weight loss in mice infected with 10^4 (light-blue squares), 10^3 (purple triangles), or 5×10^2 PFU (sky blue diamonds) of the MA10-SARS-CoV-2.

MA10-SARS-CoV-2 virus

Balb/c mice infected with 1×10^5 PFU of the MA10-SARS-CoV-2 showed significant weight loss when compared to mock-infected mice and MA-SARS-CoV-2-infected mice (Figure 2a). Moreover, the mice showed clinical signs of the disease starting two days post infection (i.e., reduced mobility and reaction time, matted fur and impaired respiration). All the MA10-SARS-CoV-2-infected mice reached the humane endpoint and had to be euthanised within four days post infection. In agreement with the observed morbidity, viral titres were significantly higher in the lung of MA10-SARS-CoV-2-infected mice as compared to MA-SARS-CoV-2-infected mice (Figure 2b).

To characterise the dose-dependent pathogenic potential of MA-SARS-CoV-2 virus, a pilot dose-ranging study was performed by infecting the mice with 10^4 , 10^3 and 5×10^2 PFU of MA10-SARS-CoV-2. Humane end-point criteria were reached in mice infected with 10^4 PFU, but not in mice infected with lower doses of 10^3 and 5×10^2 PFU. However, when compared to the mock-infected mice, all MA10-SARS-CoV-2-infected mice showed a



significant weight loss four days after infection (Figure 2c). Histologically, mice infected with the non-lethal dose of 10^3 PFU of MA10-SARS-CoV-2 displayed a moderate to severe, multifocal to coalescing, perivascular, peribronchiolar, and interstitial mononuclear infiltration, with multifocal consolidation of the lung parenchyma on day 4 post-infection (Figure 3c and f). Additionally, there was an occasional necrosis of the alveolar wall with surrounding neutrophilic infiltrates, exudation of protein-rich material into the alveolar lumen, and mild to moderate, intra-alveolar infiltrates composed of neutrophils and macrophages. Similar vascular changes to the ones described for MA-SARS-CoV-2 were also present multifocally, with concurring vessel wall disruption and moderate to severe perivascular oedema. The bronchiolar changes were comparable to the ones described for MA-infected mice.

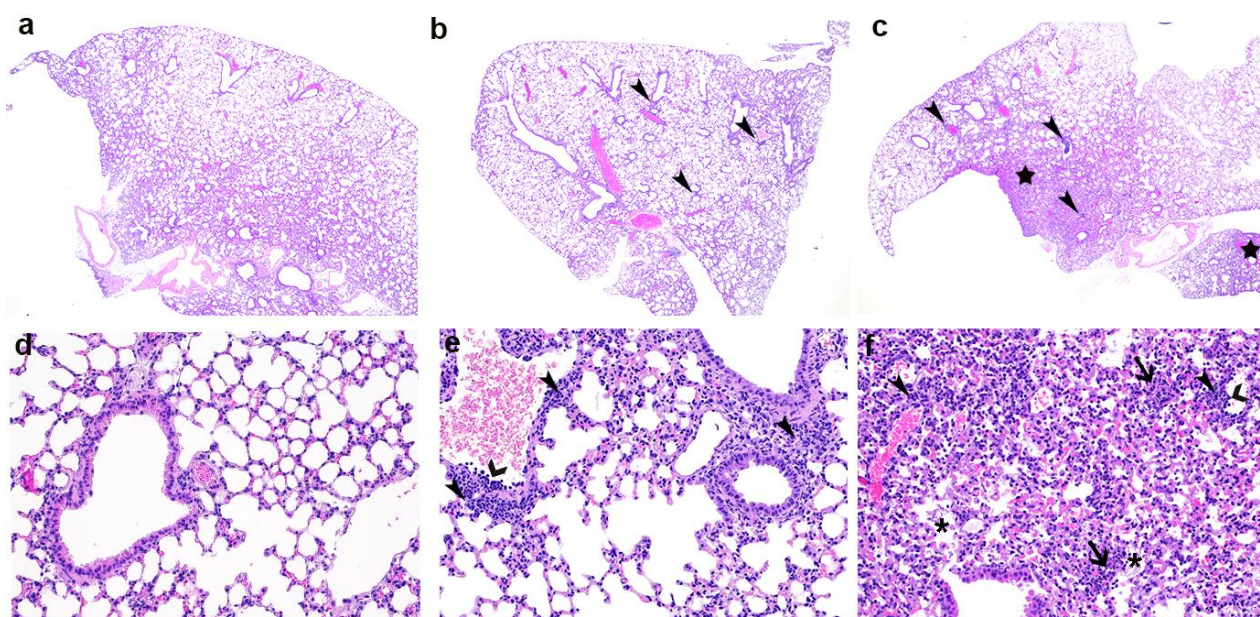


Figure 3: Histopathological findings. Mock Balb/c mice (a, d), Balb/c mice infected with 10^5 PFU of MA-SARS-CoV-2 (b,e) and 10^3 PFU of MA10-SARS-CoV-2 (c,f). In MA-infected mice, pathological lesions observed are peribronchiolar and perivascular, mononuclear infiltrates (thin arrowheads), which expand into the adjacent alveolar walls, as well as an endothelial activation and intraluminal clusters of inflammatory cells (large arrowheads). In MA10-infected mice there are increased numbers of mononuclear peribronchiolar, perivascular, and interstitial inflammatory cell infiltrates, with multifocal consolidation of the lung parenchyma (stars). Additionally, multifocal necrosis of the alveolar wall (arrows) with surrounding neutrophilic infiltration, as well as protein-rich exudation and infiltrates of macrophages and neutrophils within the alveoli (asterisks) are observed. H&E staining, upper row 20x, lower row 200x.

Discussion

We have successfully demonstrated with these experiments that the yeast TAR reverse



genetics system [6] rapidly generates mouse-adapted SARS-CoV-2 variants. These viruses despite their adaptation to mice can replicate well in Vero E6 cell lines, allowing progeny virus of sufficiently high titre to be generated for downstream experiments. On infection in mice, as reported in previous publications [1, 2], we observed similar findings in terms of high viral replication with both viruses in organs. Additionally, low pathogenicity with MA-SARS-CoV-2 and high pathogenicity with MA10-SARS-CoV-2 was also seen, confirming published data. In the context of the CARE project, both models are useful for fine-tuning during antiviral testing.

MA10-SARS-CoV-2 can replicate very efficiently using low inoculum ($<10^3$ PFU/mouse). This provides an advantage over many other animal models (humanised mice, hamsters and non-Human Primates), which all require high inoculum. Using a low inoculum provides more time for the virus to replicate and will allow a longer period for therapeutic interventions before the virus reaches a maximal load in organs.

A drawback of this approach where mutations in the Spike protein are introduced to facilitate adaptation of the virus to allow infection of mice may not reflect the ongoing evolution of viruses in the human population. Secondly, this may create a challenge for testing therapeutic antibodies, whereby a monoclonal antibody that neutralises the wild-type virus could be falsely considered as non-neutralising.

Conclusion

As the pandemic progresses, the focus of research should shift from not only concentrating on the development of vaccines but also the effort to develop prophylactic and therapeutic treatments as is the context of the CARE consortium. This model using lower virus doses has potential when assessing the efficacy of therapeutic antivirals. However, at higher doses, disease is too severe and proceeds rapidly, meaning that frequent observations of animals is required to observe differences in treatments. At the conception of this and similar projects “long COVID” had not been described therefore to date this phenomenon has been overlooked. Symptomatically “long COVID” can be described as people who have cleared the virus but continue to exhibit debilitating symptoms. As we now enter the second year of the COVID-19 pandemic these long-term effects on the population must be considered and investigated not only as a public health concern but also in terms of the damaging effects it has on the economy. This model therefore will play an important role in experiments investigating the long-term effects of SARS-CoV-2 on the lungs in animals that do not succumb to the lethal effects of the virus.

References

1. Dinnon, K.H., 3rd, et al., *A mouse-adapted model of SARS-CoV-2 to test COVID-19 countermeasures*. *Nature*, 2020. **586**(7830): p. 560-566.
2. Leist, S.R., et al., *A Mouse-Adapted SARS-CoV-2 Induces Acute Lung Injury and Mortality in Standard Laboratory Mice*. *Cell*, 2020. **183**(4): p. 1070-1085 e12.



3. Zhou, B., et al., *SARS-CoV-2 spike D614G change enhances replication and transmission*. *Nature*, 2021. **592**(7852): p. 122-127.
4. Winkler, E.S., et al., *SARS-CoV-2 infection in the lungs of human ACE2 transgenic mice causes severe inflammation, immune cell infiltration, and compromised respiratory function*. *bioRxiv*, 2020.
5. Zheng, J., et al., *COVID-19 treatments and pathogenesis including anosmia in K18-hACE2 mice*. *Nature*, 2021. **589**(7843): p. 603-607.
6. Thi Nhu Thao, T., et al., *Rapid reconstruction of SARS-CoV-2 using a synthetic genomics platform*. *Nature*, 2020. **582**(7813): p. 561-565.
7. Dietert, K., et al., *Spectrum of pathogen- and model-specific histopathologies in mouse models of acute pneumonia*. *PLoS One*, 2017. **12**(11): p. e0188251.